

Air Force Institute of Technology

AFIT Scholar

Faculty Publications

5-10-2018

Improved Space Object Detection Using Short-Exposure Image Data with Daylight Background

David J. Becker

Stephen C. Cain

Air Force Institute of Technology

Follow this and additional works at: <https://scholar.afit.edu/facpub>



Part of the [Optics Commons](#)

Recommended Citation

Becker, D. J., & Cain, S. C. (2018). Improved space object detection using short-exposure image data with daylight background. *Applied Optics*, 57(14), 3968. <https://doi.org/10.1364/AO.57.003968>

This Article is brought to you for free and open access by AFIT Scholar. It has been accepted for inclusion in Faculty Publications by an authorized administrator of AFIT Scholar. For more information, please contact richard.mansfield@afit.edu.



Accepted Author Manuscript

Journal: *Applied Optics*

Article Title: Improved space object detection using short-exposure image data with daylight background

Authors: David Becker, and Stephen Cain

Accepted for publication: 16 April 2018

Final version published: 10 May 2018

DOI: <https://doi.org/10.1364/AO.57.003968>

Access to this article is made available via **CHORUS** and subject to [OSA Publishing Terms of Use](#).

Improved space object detection using short exposure image data with daylight background

DAVID BECKER^{1*}, STEPHEN CAIN¹

¹Air Force Institute of Technology, 2950 Hobson Way, Dayton, Ohio 45433 USA

*Corresponding author: david.becker.9@us.af.mil

Received XX Month XXXX; revised XX Month, XXXX; accepted XX Month XXXX; posted XX Month XXXX (Doc. ID XXXXX); published XX Month XXXX

Space object detection is of great importance in the highly dependent yet competitive and congested space domain. Detection algorithms employed play a crucial role in fulfilling the detection component in the space situational awareness mission to detect, track, characterize and catalog unknown space objects. Many current space detection algorithms use a matched filter or a spatial correlator on long exposure data to make a detection decision at a single pixel point of a spatial image based on the assumption that the data follows a Gaussian distribution. Long exposure imaging is critical to detection performance in these algorithms, however if imaging under daylight conditions it becomes necessary to create a long exposure image as the sum of many short exposure images. This paper explores the potential to increase detection capabilities of small and dim space objects in a stack of short exposure images dominated with a bright background. The algorithm proposed in this paper improves the traditional stack and average method of forming a long exposure image by selectively removing short exposure frames of data that do not positively contribute to the overall signal to noise ratio of the averaged image. The performance of the algorithm is compared to a traditional matched filter detector using data generated in MATLAB as well as laboratory collected data. The results are illustrated on a receiver operating characteristic curve to highlight the increased probability of detection associated with the proposed algorithm.

© 2018 Optical Society of America

OCIS codes: (040.1880) Detection; (040.0040) Detectors; (100.0100) Image processing.

<http://dx.doi.org/10.1364/AO.99.099999>

1. INTRODUCTION

Safe and dependable operations in the space domain are vital to the national security interests of the United States (U.S.). According to the 2011 U.S. National Security Space Strategy, "space is vital to U.S. national security and our ability to understand emerging threats, project power globally, conduct operations, support diplomatic efforts, and enable global economic viability" [1]. In order to preserve continued space operations, the 2010 U.S. National Space Policy called out the need to fund and develop technologies to "detect, identify, and attribute actions in space that are contrary to responsible use and the long-term sustainability of the space environment" [2]. Additionally, the National Space Policy states the need to "pursue capabilities to detect, track, catalog, and characterize near-Earth objects to reduce the risk of harm to humans from an unexpected impact on our planet and to identify potentially resource-rich planetary objects".

The ability to detect and track space debris is of great concern to the National Aeronautics and Space Administration (NASA), the Department of Defense (DoD) and other space organizations around the world. Through the NASA Multiyear Authorization Act of 1990 and the NASA Authorization Act of 2005, the United States Congress mandated NASA to coordinate with the DoD and other organizations to catalogue by the year 2020, 90 percent of all asteroids and comets

larger than 140 meters that are within close trajectory of Earth [3]. Additionally, within the DoD, the ability to detect and track dim and small space objects such as nanosatellites and space debris is over particular importance to the United States Space Command (USSPACECOM) and national security. These objects pose great risk to critical space assets especially in the geostationary orbit.

The detection of asteroids, orbiting man-made objects or space debris represent similar challenges to those looking to detect, track and catalog unknown space objects. Due to their small size when viewed from a ground-based telescope, these objects are likely to be similar to an unresolvable point source on the image captured by the charge-coupled device (CCD). While these are different types of objects, ground based system within the space surveillance network (SSN) are tasked with detecting and tracking all objects which could posed a potential threat to Earth and space-based assets.

One of the factors seriously limiting space object detection assets is the inadequate telescope time available for the detection mission. Factors such as hardware upgrades, weather and maintenance all affect the amount of time available for astronomers and operators to collect data. Possibly, the greatest hindrance is the amount of prime night sky available. Imaging during twilight and daylight conditions is possible with smaller aperture telescopes but the detection algorithms are not designed for operating under these conditions. Due to the

brighter background and the limited capabilities of the CCD to not reach saturation, short exposure images become necessary. With a shorter integration time, tens to thousands of short exposure images can be captured in the time that a typical space situational awareness (SSA) asset collects a single long exposure image. Currently, processing these short exposure images relies on traditional long exposure methods such as a point detector or matched filter [4–6]. Neither of these methods are optimized to improve detection performance for short exposure imaging as they are developed using long exposure imaging in mind. Lucky imaging is a short exposure image processing technique used within the astronomical community. Significant research has delivered near diffraction limited viewing on up to 2.5m ground based telescope. However, this technique requires that a guide star be present in the image to evaluate the quality of each short exposure image [7–9]. Additionally, this method relies on registering and combining the retained images to obtain the processed image. This process is ideal for improving the resolution when imaging an object that is bright enough to easily detect.

This research is focused on improving the capability to detect dim and small space objects such as satellites and space debris to improve SSA from short exposure data obtained with current ground based electro-optic systems. The ability to detect dim objects is greatly impacted by the performance of the detection algorithm used to filter the data and decide if an unknown space object is present in the noisy scene. This paper proposes an improvement upon current detection algorithms by developing a process to selectively average multiple short exposure images to improve the signal to noise ratio (SNR) and thus improve the detection performance. Frame selection is accomplished using a two-pass approach to process the data in an effective manner while utilizing a correlation between the resulting data and the expected point spread function (PSF). Increasing the ability to detect space objects from short exposure images will increase the amount of time a telescope can be operated, provide opportunities to imaging different parts of the sky and therefore increase the number of space objects detected, tracked and then cataloged.

The proposed algorithm in this research combines a set of short exposure images that have been filtered to remove images that do not improve the correlation of the summed frames with an expected PSF. This process differs from the point detector, matched filter and lucky imaging techniques in several ways. First, minimal information is needed to apply this technique. A local guide star or reference point is not required to correlate the image with a PSF or provide a means to examine the quality of the image. Second, local registration of frames is not required. When looking for an unknown object in an image that spans an angle much larger than the tilt-isoplanatic angle, registering frames locally when no object exists in the frame results in noise spikes being registered and false alarms are identified. Gross image registration is still possible using natural guide stars, but this will not remove local motion caused by atmospheric tilt. Third, a decision on the quality of the image is made using all the frames of data in the set. This is significantly different than a lucky imaging technique which evaluates and ranks the quality of each frame individually.

The results of the frame selection short exposure correlation algorithm are compared to the performance of a spatial domain matched filter algorithm like the one used within the space community whose mission is asteroid and/or debris detection. The underlying difference lies in the way the short exposure images are averaged. Unlike a traditional approach which would involve averaging all the frames of data, the proposed algorithm discards noisy and turbulent frames of data that do not improve the overall image. The results are illustrated on a receiver operating characteristic (ROC) curve which highlights the difference in the probability of detection against the false alarm rate.

2. BACKGROUND

Established in 1984 by the University of Arizona, Spacewatch was the first program dedicated to improving the detection, tracking and then cataloging of space objects. Spacewatch has been a scientific success to the astronomical community as it was the first to use a CCD to actively scan and survey the sky in search of unknown space objects. Prior to this program, astronomers and those working in the space community were using photographic plates to image and detect objects. The use of CCDs led the program to develop the first software algorithms designed to improve space object detection in 1990 [10]. Since then, CCDs and image processing techniques have greatly improved the number of smaller and fainter space objects detected, tracked and cataloged due to significant advances in computing power, memory and storage. These advances have resulted in further research programs to develop advanced algorithms to detect faint space objects.

Traditional Space Object Detection Techniques

One of the earlier programs dedicated to improving detection algorithm was the mid-1990's Lincoln Near Earth Asteroid Research (LINEAR) program. The LINEAR algorithm developed in this program utilizes imagery obtained from a ground based electro-optic telescope to detect space objects using a binary hypothesis test (BHT) point detector [5]. Currently the SST and other assets within the SSN use a modified version of the BHT point detector developed for LINEAR to make a detection decision on a single pixel in a given frame of data. The SNR level from the point detector, shown in Eq. 1, is calculated by examining the received intensity at point, $d(x - x_0, y - y_0)$, from a single frame of windowed data. The windowed data is a $N \times N$ pixel subset of a larger image captured by the optical system. Windowing of the data allows for detection within a much smaller subset of a wide field image limiting interference from other optical sources. The windowing of the larger image decreases the number of pixels in the image being processed which significantly reduces computation time while also decreasing the likelihood that another object is in the image that must be removed prior to processing.

The point detector is a computationally simple algorithm designed to create a binary mask to identify pixels that represent an object with an intensity over a set threshold. This method of detection relies on the assumption that the data is Gaussian distributed. Thus, when the background, B , is subtracted and the result divided by the standard deviation, σ , the result is the number of standard deviations the intensity of the pixel point is from the mean.

$$SNR_{PD} = \frac{d(x_0 - y_0) - B}{\sigma} \quad (1)$$

The SNR from the point detector is the sufficient statistic used in the BHT. The two hypotheses of the BHT are the null hypothesis (H_0), that an object is not located at the tested pixel and the alternative hypothesis (H_1), that an object is located at the tested pixel point. The SNR is compared to a set threshold to determine if an object potentially exists at the tested point.

While computationally simple, the point detector's performance suffers when the intensity from the object is not in a single pixel of the detector. The intensity of the object can be spread across multiple pixels due to several factors including atmospheric turbulence, diffraction and geometrical aberrations in the optical system. This reduces the intensity in the tested pixel and a lower SNR that adversely degrades the performance of an algorithm dependent on testing each individual pixel point. To improve the probability of false alarms, the SST utilizes a modified version of the LINEAR algorithm across multiple frames of data to detect unknown space objects [11]. The LINEAR algorithm implemented by SST requires 3 successful

detections from independent frames before the data is handed off for further processing and confirming an objects existence.

More computationally complex algorithms known as matched filter or correlation algorithms have been developed to improve space object detection performance. This algorithm is used by the highly successful Pan-STARRS telescope for making space object detection decisions [12]. A matched filter approach is based on matching the observed data with the expected PSF. The expected PSF can be determined from measurable statistical parameters of the atmosphere or can be measured by viewing a nearby star [13]. This approach assumes that the object is either small or far away enough that it is essentially a point source when viewed through the optical system. The expected PSF is correlated with the data to determine if an object is present at a given pixel point. However, unlike the point source detector, multiple pixels are used to make a detection decision. A standard matched filter algorithm, shown in Eq. 2, is implemented in the SExtractor software suite which is largely used within the SSA community for object detection, measuring and classifying objects from astronomical images [14]. The detection piece of this program is a matched filter designed to detect faint space objects assuming Gaussian distributed noise by correlating the data with the expected PSF and dividing by the standard deviation, σ_{MF} , of the noise in the $N \times N$ pixel region. The value calculated by the matched filter in Eqs. 2 and 3, SNR_{MF} , is the sufficient statistic compared to a threshold in a BHT to make a detection decision.

$$SNR_{MF} = \frac{\sum_x \sum_y (d(x-x_0, y-y_0) - B)h(x,y)}{\sigma_{MF}} \quad (2)$$

$$\sigma_{MF} = \frac{1}{N^2} \sqrt{\sum_x \sum_y (d(x-x_0, y-y_0) - B)^2} \quad (3)$$

Short Exposure Imaging Techniques

Each of the previously discussed detection algorithms are designed for utilizing long exposure data with traditionally low background light. A long exposure image is generally used because it allows a lower SNR object to be detected while averaging out lower order atmospheric turbulence and random spikes in intensity due to the Poisson nature of the photons received. However, under a daylight imaging scenario, the background will be dominate in the image and the intensity of the object appears to be lost in the background light. Short exposure imaging becomes necessary to avoid saturation in the image due to the limited depth of the camera pixel wells and the sheer number of photons arriving during longer integration times in daylight conditions. While there is limited research in detection of space objects using daylight imaging, short exposure imaging is not a new area of research. Lucky imaging is a post-processing technique used broadly within the astronomical community to obtain near diffraction limited images from ground based telescopes through the use of short exposure imaging [8, 9, 14-16].

Short exposure imaging is typically utilized for image reconstruction and for obtaining higher resolution imaging from ground-based telescopes. When many frames of data are taken over the course of a single long exposure image time frame the atmosphere over each image is essentially frozen. The brief integration time allows for some images in a set to obtain near diffraction limited viewing conditions since the lower order aberrations such as tip and tilt are not averaged in that time instance. The freezing of the atmosphere over this short time period allows photons to remain concentrated on the CCD. When a select number of these images are registered and combined the result is an increase in the resolution of the combined image. Using the

lucky imaging technique with a point source object or a guide star in the image frame, a metric such as the Strehl ratio is used to evaluate the quality or sharpness of each individual frame of data. A defined percentage of "bad" frames are removed from the ensemble of short exposure images. The remaining frames are then registered and combined to achieve an improved image [7]. The lucky imaging technique can provide significant improvements to spatial resolution under the right conditions and with the appropriate hardware. However, under daylight imaging of dim objects the technique loses its advantage since the objects SNR is too low for the daylight background and there is no obvious object in the image. As a result, the technique fails to have an object to register and tends to register random noise spikes in the frame if a low SNR object exist in the image or not. Additionally, this technique is difficult to implement in a sky scan and detect mission. Under typical conditions, lucky imaging has an isoplanatic patch of nearly 1 arcminute or 0.01667 degrees [18]. In order to scan and detect a 90-degree portion of the sky would require 5400² images using the lucky technique with a guide star. This number of images would far exceed the time available for the telescope to capture in a given night.

A significant drawback to short exposure imaging is that the shorter integration time means fewer photons will be measured by the CCD. This fault is typically overcome by averaging together many frames of data to essentially obtain a long exposure image. The Poisson photon noise statistics of the averaged image will be comparable to the sum of the short exposure images since the sum of multiple Poisson random variables is itself a Poisson random variable with a rate parameter equal to the sum of the individual rates [16]. An issue with averaging many short exposure images in traditional night time imaging scenarios is detector noise which accumulates as frames are averaged together. Unlike photon noise, Gaussian distributed detector noise is not signal dependent and is a result of the detector and readout electronics [16, 19].

As the number of expected photons decreases for shorter integration times, the detector noise variance, σ_n^2 , becomes significant compared to the Poisson rate parameter, \bar{K} . When P frames of data are averaged together, the detector noise variance follows Gaussian statistics and is a function of the number of frames averaged and the readout noise variance.

$$var\{d(x, y)\} = P\bar{K} + P\sigma_n^2 \quad (5)$$

Under a daylight imaging scenario, the expected number of photons is significantly large enough even under short exposure integration times that the readout noise becomes insignificant in the received image.

Atmospheric Model

In many SSA ground based telescope systems, the integration time is significantly long enough that it operates in the long exposure regime. The long exposure PSF and optical transfer function (OTF) are used to model the average size and spatial frequency content of a point source object viewed through a telescope [13]. The long exposure OTF for a circular aperture telescope is defined as

$$H_L(f_x, f_y) = \exp\left[\left(\frac{\bar{\lambda}z\sqrt{f_x^2 + f_y^2}}{r_0}\right)^{5/3}\right]. \quad (4)$$

Where $\bar{\lambda}$ is the mean wavelength, z is the telescope focal length and f_x and f_y are spatial frequencies in the OTF. The Fried atmospheric seeing parameter, r_0 , is a measure of the quality of optical propagations

through the atmosphere [20]. Values of 5-15 cm are realistic for most operational sites. As defined in Eq. 5, the long exposure OTF can be converted into the spatial domain to obtain the long exposure PSF, $h(x, y)$, using the inverse Fourier transform of the OTF. This represents the spatial image expected when viewing a distant point source.

$$h(x, y) = \mathfrak{F}^{-1}\{H_L(f_x, f_y)\} \quad (5)$$

The long exposure PSF averages the random phase fluctuations due to the atmosphere to produce a spatially large PSF. On average, a long exposure PSF will contain zero tilt and will be an even and symmetric function.

Background Light

Background noise is the result of any light or signal aside from the light propagating from the object that is measured by the detector. There are various sources of background noise and many are dependent on the situation, they include but are not limited to the sun, starlight and building or city lights reflecting off other surfaces and captured by the primary mirror of the telescope. The background light, B , can be estimated during data capture via post-processing by taking the median value of all N pixels in each dimension of the windowed data, $d(x, y)$.

$$B = \text{median}(d(x, y) \forall (x, y) \in [1, N]) \quad (6)$$

3. ALGORITHM DEVELOPMENT

Space object detection algorithms utilize both single and multiple spatial images obtained from ground-based telescopes. Many SSA platforms use multiple frames in their processing chain, however they begin with being able to detect on a single frame and use the multiple frames of follow-up data to confirm or reject the detection decision. Additionally, multiple frames can be tested to reduce the false alarm rate to an acceptable level. This research is focused on improving the ability to detect a dim space object from a single frame of data so that detection can be passed on to further multi-frame analysis techniques and follow-up analysis. The detection process chain sometimes includes some amount of pre-processing of the data to do tasks such as measure background, discard faulty pixels or remove known objects from the image using telescope pointing information and a celestial map [11].

Due to the bright sky background associated with daylight imaging, the data will be limited to short exposure images that must be processed for object detection. This algorithm takes advantage of the short exposure atmospheric turbulence to improve the SNR of the data. The data is divided into subsets of 10 frames that will be processed together to emulate a camera imaging at a rate of 10 frames a second. This short time is chosen to reflect the fact that sky surveys looking for new objects must scan the sky in a reasonable amount of time. Instead of simply stacking the images to obtain a higher SNR image, the images are processed and stacked in a manner that further increases the SNR and improves detection performance. This process removes frames of data in the subset that do not contribute to improving the stacked image. Due to the need for multiple frames, each iteration of this algorithm would not achieve real time rates however it could operate in near real time.

The first step in the daylight space object detection algorithm is to start with a modified version of the matched filter detection method used with long exposure data. An estimate of the background, B , is obtained by calculating the median value for all pixels in the windowed data, this estimated background is removed from the data. The algorithm processes the 10 frames of data in each iteration. This first process removes each individual frame one at a time, averages the

remaining frames and convolutes the summed images with the PSF. The convolution of each k^{th} removed summed image and the PSF, $h(x, y)$ is calculated from Eq. 7, resulting in SNR values for each k^{th} frame of data, $Q_{FS}(n)$. This is implemented in the Fourier domain as the multiplication of the Fourier transformed data and the OTF, H_L . The flow of this initial processing is illustrated in Fig. 1. After each frame has been removed and a new value is calculated the values are ranked in descending order. This translates to ranking which frames when removed from the average and convoluted with the PSF decrease the SNR the most significantly.

$$Q_{FS}(n) = \sum_{k=1, k \neq n}^{10} (d_k(x, y) - B) * h(x, y) \quad (7)$$

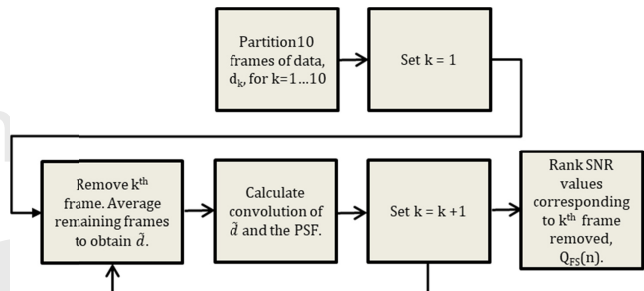


Fig. 1. Flow chart of initial processing completed in the short exposure frame selection algorithm.

With the ranked frames, the algorithm then processes the 10 data frames by removing the one that most significantly decreased the SNR and calculating the new average correlated SNR of the remaining frames using the match filter from Eq. 2. As each poor frame is removed, the correlation between the PSF and the averaged data increases. The algorithm continues to remove frames in descending order until the computed average SNR fails to increase from the last iteration. Once the SNR has reached its peak the algorithm stops removing frames of data. This process differs from the initial processing step in that it is removing frames the least viable frames first and then computing the SNR. It is important to note that the initial process doesn't factor in where the peak of the convolution occurs. This becomes apparent in the H_0 case were the algorithm would pick up on noise fluctuations. This secondary correlation test if the object is at the pixel location being tested. At no time are the individual frames registered prior to averaging them together.

The process would seem to be counterintuitive, that throwing away data would increase the likelihood of detection using short exposure data. However, under atmospheric conditions, averaging noisy or highly distorted image data could potentially result in a lower SNR image due to the unpredictability of lower order atmospheric aberrations in short exposure image. This process removes frames that do not collectively contribute to improving the SNR of the data. Collecting data using this method requires significantly higher data transfer rates as ten to thousands of short exposure images can be captured in the typical long exposure time frame.

To properly evaluate the performance of this algorithm, the exact same script must be used for H_1 and H_0 data sets. The MATLAB script for processing this data only requires the captured data set and doesn't require any preset information outside of the expected PSF. The expected PSF can be obtained by imaging a nearby star or estimated from system parameters and a measurement of the seeing parameter, r_0 , using the long exposure PSF formula given in Eq. 5 [13]. While the data collected is defined as short exposure, the long exposure PSF

model is used since the individual frames of data are averaged together prior to correlation to create an effective long exposure image.

4. SIMULATION AND EXPERIMENTAL DATA

Simulated and experimental data were used to analyze the performance of the proposed space object detection algorithm. This section describes the setup used to collect the two data sets in detail.

In practice, it is likely that a wide field of view (FOV) camera capturing data on a telescope will contain many thousands of objects. These objects will include stars, satellites and potentially space debris and will all have varying levels of intensity. These objects are treated identically by the algorithm since they would appear as point sources to the optical system. Additionally, the frame of data collected by the optical system is reduced to only test a small subset of the entire frame. This increases the likelihood that multiple objects do not exist within the subset windowed data while decreasing the computational complexity involved in processing large frames of data. This approach is used with other space object detection algorithms. The data collected from the SST contains 6144×4096 pixels, however subsets as low as 15×15 are used in object detection algorithms. A window of this size allows for a PSF to be contained within the window while providing enough pixels for the background statistics to be calculated. Operationally, the 15×15 window would slide across the entire image as each individual pixel was tested. The data used for testing this algorithm was set at 20×20 pixels. Outside of computation time and possible interference from other objects, there is no reason that a larger window could not be chosen [22].

Simulated Data

The simulated data was developed in MATLAB to mimic a single point source object within the data frame. The parameters used in the simulation are summarized in Table 1. The use of MATLAB to create data allows the ability to simulate accurate statistical distributions and create realistic looking data while removing unknown variables in the scenario. Removing these unknown variables limits the data to investigate only the scope of the proposed algorithm. Images were simulated under both the hypothesis that an object is present at the pixel location being tested and that no object is present in the scene, see Fig. 2. Under the H_1 hypothesis, an object exists at the tested pixel location, (x_0, y_0) . The intensity of the object can be varied to test the algorithm at various SNR levels. Under the H_0 hypothesis, no object exists in the scene. This is simulated using the same statistical assumptions for background light and the atmosphere except the intensity of the object is set to zero. Accurate short and long exposure PSF statistics were incorporated based on correlated turbulence models [23] and built-in Poisson random variable functions were used to simulate accurate statistical distributions for the background noise. The model for the PSF was generated using Equation (4).

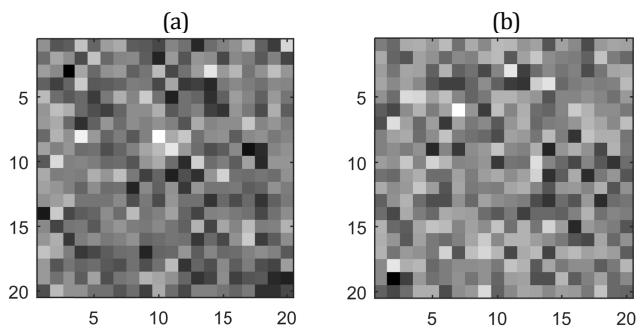


Fig. 2. Single frame of data simulated in MATLAB using accurate turbulence and noise models. (a) Object present (H_1). (b) No Object present (H_0).

Table 1. System and Data Parameters Used in MATLAB Simulation

Parameter	Value
Primary Aperture Diameter, D	0.10 m
Seeing Parameter, r_0	0.05 m
Number of Frames Simulated	10000
Window Size, N	20×20 pixels
Background Photon Count, B	10,000 photons
Target Intensity, θ	1,500 photons

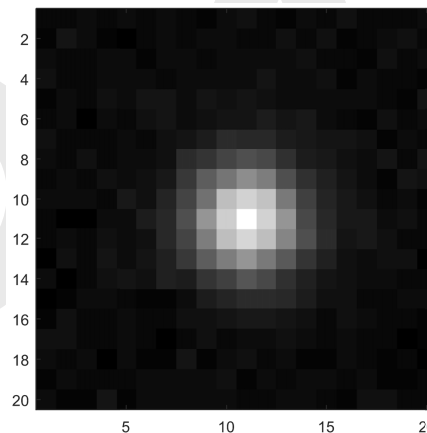


Fig. 3. Simulated point spread function (PSF) used in the algorithm.

Experimental Data

Experimental data was collected using a hybrid approach in an optics laboratory. A camera, aperture stop and focusing lens were set up on an optical bench to capture frames of data. A hot air fan was used in the optical path to induce random atmospheric turbulence in the scene. A light emitting diode (LED) behind a 75-micron pinhole was placed in focus with the detector after reflecting off a mirror half way down the path using a 500mm lens. A computer screen was placed out of focus behind the mirror to provide an adjustable background light source. This hybrid approach allowed for producing a point source object with a bright background at varying SNR levels. Using this approach removes the entirely simulated environment and provides randomness to collected data while allowing for ease in adjusting the intensity of the background compared to the point source object.

To collect H_1 data, the MATLAB displayed image was adjusted to a 256-grayscale image with the background level set to $\frac{3}{4}$ the brightness of the object and the LED turned on to represent the object. This

provided nearly 10000 counts of background light on the laboratory detector. 1000 short exposure images were collected with the camera integration time set to 100ms. Similarly, 1000 frames of H_0 data was collected with the same intensity level for the background except the LED is turned off. An example of the collected data under each hypothesis is shown in Fig. 4. The parameters for the experimental data collected in the lab is summarized in Table 1.

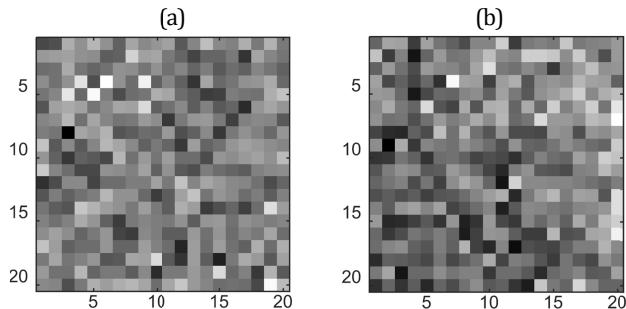


Fig. 4. Single frame of experimental data collected in the optics laboratory. (a) Object present (H_1). (b) No Object present (H_0).

The long exposure PSF of the optical system is needed by the algorithm for object detection. This was experimentally collected by setting the monitor to a black background with a single illuminated pixel. The camera was integrated for 1 second to obtain the long exposure PSF, shown in **Error! Reference source not found.** This PSF was used for correlating with the frame selected data in the algorithm. One observation noted is the smaller PSF in the experimental data compared to the simulation. This is due to the larger sampling of the data in the CCD. This binning of data effectively reduces the size of the PSF and object footprint on the CCD. However, this has no effect on the algorithm since the PSF is an accurate model of the expected data under the H_1 hypothesis.

Table 2. Experimental Data Collection Setup & Parameters

Parameter	Value
Camera	ThorLabs 8050M-GE-TE
Integration Time	100 ms
Display	Dell UltraSharp U2410
Display Pixel Pitch	0.27 mm
Focusing Lens	500 mm
LED Pinhole Size	75-micron
Number of Frames Collected	1000
Window Size, N	20 x 20 pixels
Average Background Count, B	10,097 counts

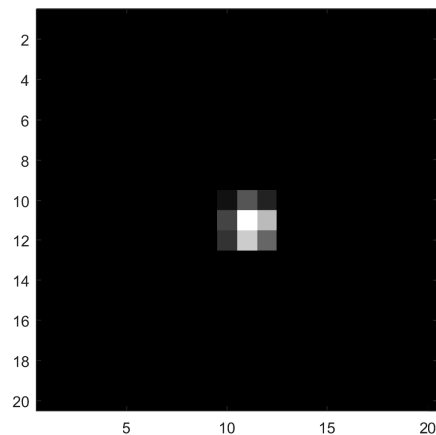


Fig. 5. Experimental laboratory data collect of the point spread function (PSF) used in the algorithm.

5. RESULTS AND ANALYSIS

The performance of the detection algorithm is defined by its ability to maintain an acceptable amount of false alarms while logging detections. Two terms are typically used to describe this process. The probability of detection, P_D , is the probability of correctly determining that an object is present at a given location whereas the probability of false alarm, P_F , is the probability that the algorithm determines an object is present at the tested pixel location when there is no object truly present. The P_F is usually set to an extremely low level that is acceptable to meet mission and resource constraints since there are potentially millions of pixels to test in a single frame and each detection requires resource demanding follow-up analysis. When considering that a single frame of data from the SST contains over 25 million pixels, a false alarm rate of 10^{-9} is standard.

Receiver Operating Characteristic Curve

A ROC curve is a method used to illustrate the P_D and P_F . The ROC curve doesn't require a specific detection threshold to be set. Instead, the P_D and P_F are both calculated for the full range of threshold values that result in detection and false alarm probabilities between zero and one. The ROC curve is built by modeling the SNR values from the algorithms test data as Gaussian random variables. The mean and variance of the test statistic can then be used to generate the detection and false alarm probabilities using a Gaussian PDF. The upper right corner of the ROC curve represents the performance of the algorithms as the threshold is lowered. There is a point in this region where the traditional matched filter outperforms the proposed algorithm. In this region, the false alarm rate is significantly higher and above levels used in operation.

Using the simulated data, the performance of the new algorithm proposed in this paper was compared to both a traditional matched filter approach and a lucky imaging technique. Under the traditional matched filter, the 10 frames of data are averaged together, no frames are removed, and the data is correlated with the expected PSF and calculates the SNR using the matched filter from Eq. 2. The lucky imaging technique was set with a selection rate of 40%. The best 4 frames of data are selected using the Strehl ratio as a quality metric, these frames were registered and averaged. The ROC curves for the simulated and experimental data are shown in Fig. 6 and Fig. 7. The

ROC curve using the simulated data illustrates the difficulty the lucky technique encounters with low SNR objects. Selection rates of 10 and 20% were also attempted with the lucky imaging technique but produced even worse results. Based on the simulated results, only the traditional matched filter and new frame selection algorithm were examined with experimental data. The results from both of the ROC curves show a significant P_D increase for a given P_F when operating in the low SNR regime for the new frame selection algorithm. The low SNR can be predicted by examining the data in Fig. 2 and Fig. 4 and seen by the extremely low detection probability for a $P_F \approx 10^{-9}$. At this operational level of false alarm, the frame selection algorithm shows a nearly 20% improvement in the P_D .

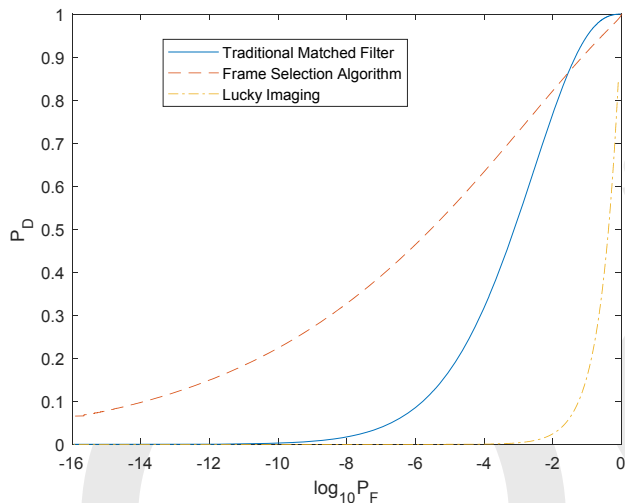


Fig. 6. Simulated Data - ROC curves for the traditional matched filter, frame selection algorithm and lucky imaging technique using 10 frames of data.

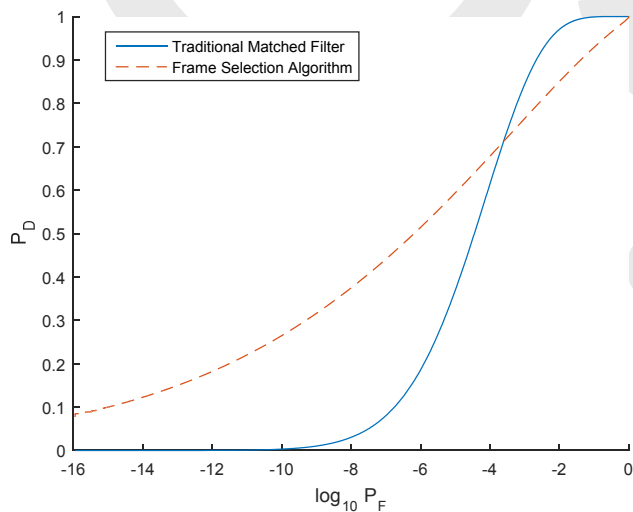


Fig. 7. Experimental Data - ROC curves for the traditional matched filter and the frame selection algorithm each using 10 frames of data.

6. CONCLUSIONS

This paper presents a method to improve the probability of detecting dim or low SNR space objects in images obtained during bright sky daylight conditions. Under daylight imaging conditions, it is required to reduce the integration time of the sensor down to short exposure

time intervals to accommodate the increased number of photons arriving at the CCD and the limited well depth. Two techniques for post-processed object detection were examined and compared to the proposed algorithm. First, a matched filter algorithm approach using a single frame of data obtained by averaging the individual frames. Second, a lucky imaging approach was examined that selects a portion of the short exposure frames based on their quality which are then registered and combined. The proposed algorithm takes into account that under short exposure conditions there will be time instances that result in excellent viewing and times when the atmosphere is particularly poor, and the image is greatly distorted. The algorithm iteratively removed frames to generate a higher SNR image which results in increased detection probabilities. Unique to this approach is that the PSF of the object is not required for correlating or for using as a reference in evaluating the quality of each individual short exposure image. The entire set of short exposure images is used to reject frames that don't improve the quality of the combined image. Additionally, image registration is not utilized due to the assumed low SNR of the object. This results in a lower false alarm rate as noise spikes are not registered and combined to create a false object.

Using both simulated and experimental data, the algorithm demonstrated the ability to significantly improve the probability of detection by 15-30% for low SNR objects while maintaining low false alarm rates. This could potentially result in a significant number of new detections found if implemented using current SSA systems.

This approach does require short exposure imaging with hardware that would require higher frame rates. The sensor must output significantly more frames of data in the same time as a single image frame. The higher frame rate can result in significantly greater readout noise when averaging the frame together. Under daylight imaging, this is mitigated due to high photon counting noise becoming the dominating noise source. It is possible that this algorithm's approach would be feasible under traditional night sky imaging if additive noise from the detector, camera's readout electronics and dark current was significantly less than the noise induced by the background or if the object was significantly bright. However, current algorithms already work well with high SNR object.

With an increase in the number of assets launched into space, the need to improve our detection and tracking of harmful objects will only increase as well. It is likely this will further constrain tight budgets and operators time with telescope assets. The potential to improve the detection capability of imaging in the daylight could mitigate some of these issues while providing newer areas of the sky to scan and an increased number of object detections.

Future research focused on refining the frame selection process to better select frames would increase the correlated SNR. This would increase the performance of the algorithm. Additionally, this algorithm can be tested using data obtained from a SSN sensor for further testing and evaluation.

Funding. Air Force Office of Scientific Research (AFOSR).

Acknowledgment. The views expressed are those of the authors and do not reflect the official policy or position of the Department of Defense or the U.S. Government.

References

1. US Department of Defense and Office of the Director of National Defense, "National Security Space Strategy Unclassified Summary," p. 14, 2011.
2. Office of the President of the United States of America, "National Space Policy of the United States of America," *United States Gov.*, p. 18, 2010.

3. U. Congress, *National Aeronautics and Space Administration Authorization Act of 2005*. U.S. Congress, 2005, pp. 2135–2321.
4. S. C. Pohlig, “An Algorithm for Detection of Moving Optical Targets,” *IEEE Trans. Aerosp. Electron. Syst.*, vol. 25, no. 1, pp. 56–63, 1989.
5. H. Vigh, G. Stokes, F. Shelly, M. Blythe, and J. Stuart, “Applying Electro-Optical Space Surveillance Technology to Asteroid Search and Detection: The LINEAR Program Results,” *Sp. 98*, pp. 373–381, 1998.
6. J. Chris Zingarelli, Eric Pearce, Richard Lambour, Travis Blake, Curtis J. R. Peterson, and Stephen Cain, “Improving the Space Surveillance Telescope’s Performance Using Multi-Hypothesis Testing,” *The Astronomical Journal*, Vol. 147, No. 5, pp. 111–121 (May 2014)
7. C. Mackay, “High-efficiency lucky imaging,” *Mon. Not. R. Astron. Soc.*, vol. 432, no. 1, pp. 702–710, 2013.
8. N. M. Law, C. D. Mackay, and J. E. Baldwin, “Lucky Imaging: High Angular Resolution Imaging in the Visible from the Ground,” *Astron. Astrophys.*, vol. 446, pp. 739–745, 2005.
9. J.-L. Nieto and E. Thouvenot, “Recentring and selection of short-exposure images with photon-counting detectors,” *Astron. Astrophys.*, vol. 241, no. 2, pp. 663–672, 1991.
10. “Spacewatch Project, <http://spacewatch.lpl.arizona.edu/>.” [Online]. Available: <http://spacewatch.lpl.arizona.edu/>. [Accessed: 26-Oct-2016].
11. J. D. Ruprecht, J. S. Stuart, D. F. Woods, and R. Y. Shah, “Detecting small asteroids with the Space Surveillance Telescope,” *Icarus*, vol. 239, pp. 253–259, 2014.
12. “Pan-STARRS, <http://pan-starrs.ifa.hawaii.edu/public/home.html>.” [Online]. Available: <http://pan-starrs.ifa.hawaii.edu/public/home.html>. [Accessed: 16-Nov-2016].
13. J. W. Goodman, *Statistical Optics*. New York: John Wiley & Sons, Inc., 2000.
14. E. Bertin and S. Arnouts, “SExtractor: Software for source extraction,” *Astron. Astrophys. Suppl. Ser.*, vol. 117, no. 2, pp. 393–404, 1996.
15. A. Macdonald, “BLIND DECONVOLUTION OF ANISOPLANATIC IMAGES COLLECTED BY A PARTIALLY COHERENT IMAGING SYSTEM,” Air Force Institute of Technology, 2006.
16. M. Roggemann and B. Welsh, *Imaging Through Turbulence*. Boca Raton, FL: CRC Press, 1996.
17. D. L. Fried, “Probability of getting a lucky short-exposure image through turbulence*,” *J. Opt. Soc. Am.*, vol. 68, no. 12, p. 1651, 1978.
18. C. Mackay, “High-Resolution Imaging with Large Ground-Based Telescopes,” *OPN Opt. Photonics News*, pp. 22–27, 2009.
19. S. C. Cain and R. D. Richmond, *Direct-Detection LADAR Systems*. SPIE Publications, 2010.
20. D. L. Fried, “Optical Resolution Through a Randomly Inhomogeneous Medium for Very Long and Very Short Exposures,” *J. Opt. Soc. Am.*, vol. 56, no. 10, p. 1372, 1966.
21. D. Woods *et al.*, “The Space Surveillance Telescope: Focus and Alignment of a Three Mirror Telescope,” in *Advanced Maui Optical and Space Surveillance Technologies Conference*, 2012.
22. Tyler Hardy, Stephen Cain, Jae Jeon, and Travis Blake, “Improving space domain awareness through unequal-cost multiple hypothesis testing in the space surveillance telescope,” *Applied Optics*, Vol. 54, Issue 17, pp. 5481–5494, (2015)
23. I. Putnam, “Atmospheric Impact on Long Pulse Laser Detection and Ranging (LADAR) Systems,” Air Force Institute of Technology, 2013.

Published by

